# The effects of the pulsatile period on the size of recirculation bubble in the vicinity of stent struts

**B Jiang[1], V Thondapu[1,2], P Barlis[1,2], E K W Poon[1] and A S H Ooi[1]**

[1] Department of Mechanical Engineering, Melbourne School of Engineering, The University of Melbourne, Victoria 3010, Australia
[2] Department of Medicine, Faculty of Medicine, Dentistry & Health Sciences, The University of Melbourne, Victoria 3010, Australia

Corresponding author: b.jiang1@student.unimelb.edu.au (B. Jiang)

**Abstract**. Incomplete stent apposition (ISA) is sometimes found in stent deployment at complex lesions, and it is considered to be one of the causes of post-stenting complications, such as late stent thrombosis and restenosis. The presence of ISA leads to large recirculation bubbles behind the stent struts, which can reduce shear stress at the arterial wall that retards neointimal formation process and thus lead to complications. Computational fluid dynamics (CFD) simulations are performed on simplified two-dimensional axisymmetric arterial models with stents struts of square and circular cross-sectional shapes at a malapposition distance of 120 μm from the arterial wall. To investigate the effects of pulsatile flow period on the dynamics of the recirculation bubbles, high fidelity simulations are carried out with pulsatile flows of period 0.4 s and 0.8 s. Under the condition of the same flow rate, both square and circular strut cases show that shorter period provides greater flow deceleration, leading to the formation of a larger recirculation bubble. With the same thickness, circular strut has a significant improvement over the square strut in terms of the size of the recirculation bubble, and therefore less likely to lead to complications.

## 1. Introduction

Stenting has been a common intervention treatment for stenosis. Intracoronary stent design has evolved from bare metal stents (BMS) to drug eluting stents (DES) and bioresorbable vascular scaffolds (BVS) over the past 30 years in order to reduce adverse clinical outcomes such as in-stent restenosis (ISR) and stent thrombosis (ST) [1]. However, incomplete stent apposition (ISA) remains common for stent deployment around complex lesions and is considered to be a major cause of post stent complications. In particular, very late ST is often associated with patients who has DES deployed [1].

The presence of malapposed struts influences local haemodynamics, and together with the pulsating effect the human heart recirculation bubbles distal to stent strut are often generated during rapid flow deceleration in a cardiac cycle. These recirculation bubbles slow down local blood flow velocity and yield a lower wall shear stress (WSS) [2]. Low WSS (<0.5 Pa) provides an environment for pro-inflammatory and procoagulant elements to reside longer and leads to less conductivity of endothelialisation [3]. Hence, the long-term outcomes of ISA are possible ISR and/or ST. In this study, we employ computational fluid dynamics (CFD) simulations to show that the size of the

recirculation bubble is correlated to the pulsatile nature of the coronary flow (specifically during rapid flow deceleration) and the cross-sectional shapes of the struts.

## 2. Methodology

Figure 1 (a) presents a commonly available stent model implanted in a 3 mm diameter cylindrical tube. The cylindrical tube represents an idealised segment of the left anterior descending (LAD) artery with an average diameter of 3 mm [4]. We further simplified this axisymmetric stent model into cylindrical ring with both square and circular cross-sections for analyses (see Figure 1(b)) and hence reducing computational expense via performing 2-dimensional axisymmetric CFD calculations (see Figure 1b). We considered stent struts of 120 μm thick, a common thickness of commercial drug-eluting stent strut [1] and a moderate malapposition distance (MD) to be 120 μm [5].

CFD simulations were carried out by directly solving the incompressible Navier–Stokes equations using an open source CFD software, OpenFOAM-2.1.1 (OpenCFD Ltd., ESI group, Bracknell, UK). The temporal term was discretised using a backward Euler scheme whereas standard Gauss linear was used for gradient terms. Gauss linear upwind and Gauss linear corrected discretisation schemes were applied to divergence and Laplacian terms, respectively. Velocity and pressure were coupled through a standard PISO algorithm with a time step of $1\times10^{-5}$ s.

Blood was assumed to be Newtonian with a density of 1000 kg/m$^3$, and dynamic viscosity of $2.5\times10^{-3}$ Pa·s. In order to capture the boundary layer characteristic near to arterial wall and strut surface, hexahedral elements were cluster to the arterial wall and strut surface (see Figure 1(c)) (first cell element is 7.5 μm normal to the strut surface in square strut model; 6.73 μm in circular strut model). A grid resolution study was performed by quadrupling the number of hexahedral elements, and no significant difference was found in terms of important haemodynamic metrics.

Pulsatile coronary flow velocity from the LAD [6] was applied at the inlet of the axisymmetric domain. A zero-pressure boundary condition was employed at the outlet. The arterial wall and the stent strut surface were assumed to be rigid and non-slip and wedges boundary condition was applied to the remaining patches of the computational domain. The mean blood flow rate was kept constant at 1.3 ml/s (which corresponds to approximately 0.1839 m/s) in this study while increasing the cardiac cycle from 0.4 s and 0.8 s (see Figure 1 (d)). This corresponds to Reynolds number with respect to the arterial diameter, $Re_D = U\cdot D/\nu$, from 107 to 342 throughout the cardiac cycle, and Reynolds number corresponding to the stent strut thickness, $Re_T = U\cdot T/\nu$, from 4.3 to 13.7, where U is the instantaneous inlet velocity, ν is kinematic viscosity, D is arterial diameter and T is the strut thickness.

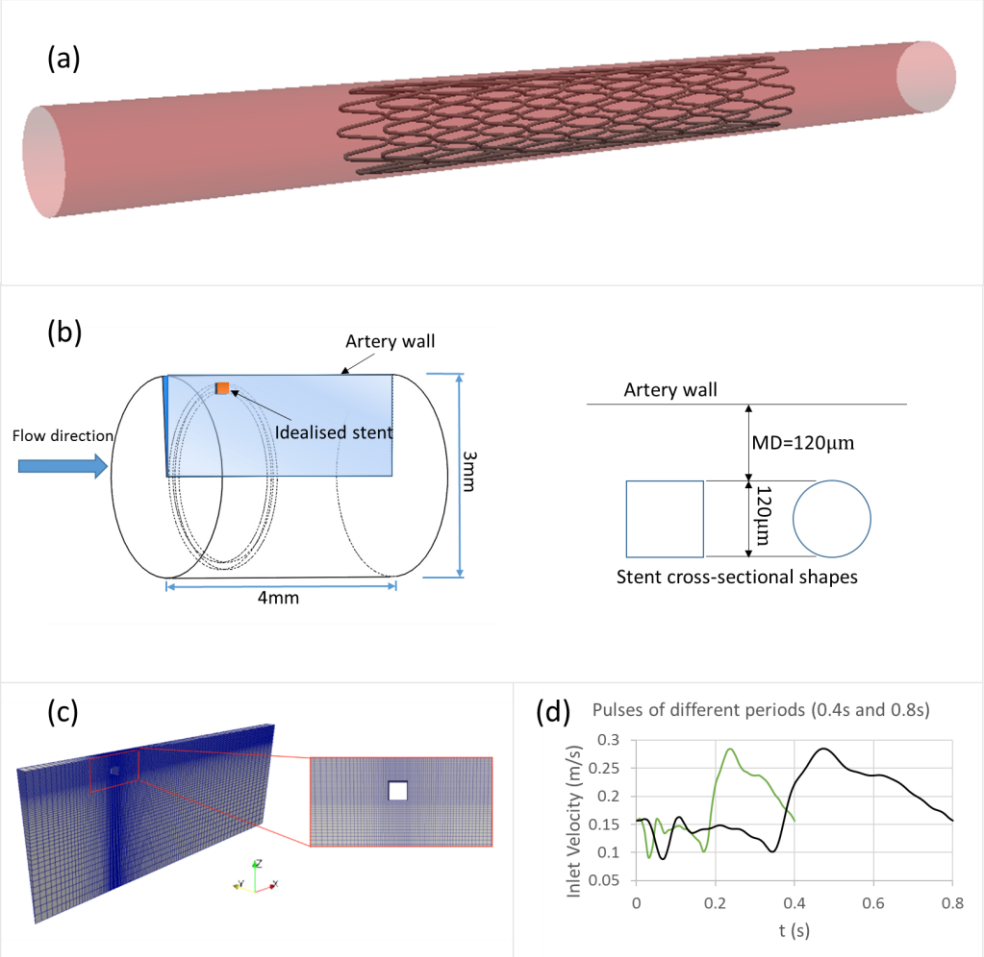


**Figure 1.** (a) A demonstration of a commonly available stent placed in an idealised segment of a coronary artery. (b) Simplified computation model of the malapposed stent in the idealised arterial geometry for CFD analyses and dimensions of the square and circular cross-sectional stent strut. (c) 2D axisymmetric model (in wedge shape) was generated and hexahedral elements density was increased near the arterial wall and strut surface. (d) A pulsatile coronary flow velocity from the LAD was applied to the inlet of the computational domain as shown in (c). Two different cardiac cycles (0.4 s and 0.8 s) were being considered.

## 3. Results and discussion

The temporal evolution of recirculation bubble distal to the malapposed strut was studied at various points in time for pulsatile flow with cardiac cycle of 0.4 s and 0.8 s. To ensure that all initial transients have convected out of the computational domain, the simulations were carried out for two cardiac cycles but only the data from the second cycle were used in the analyses below.

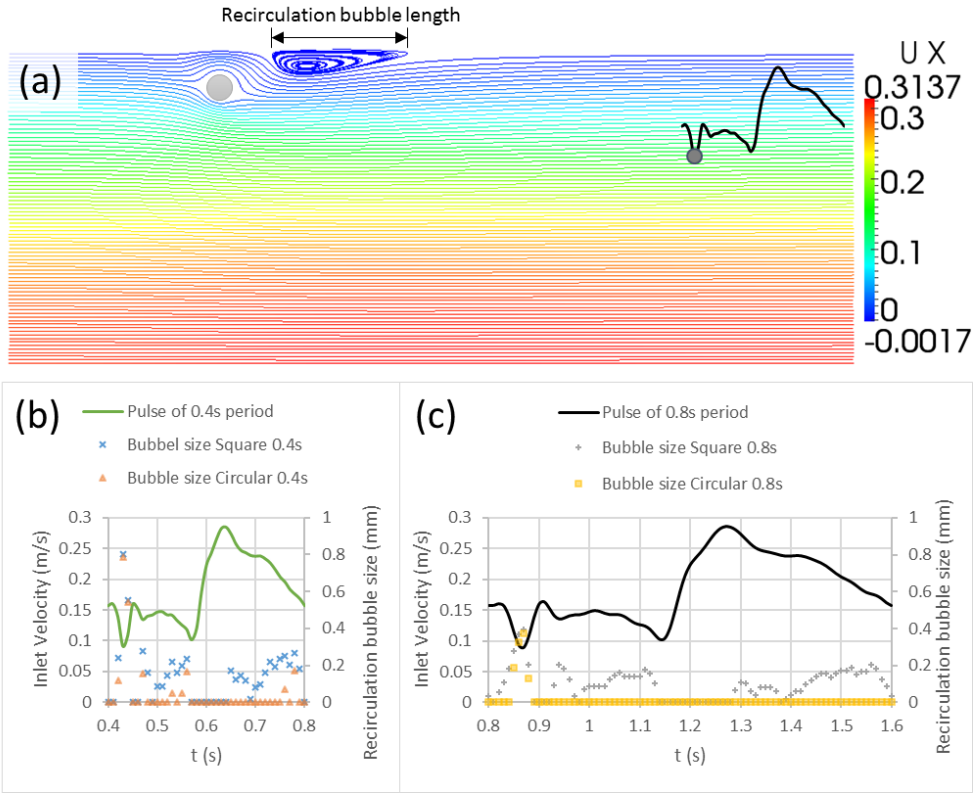


**Figure 2.** (a) The location and size of the streamline recirculation bubble distal to the malapposed stent strut. (b) & (c) Evolution of the size of the recirculation bubble distal to a malapposed strut (both square and circular cross-section) throughout a cardiac cycle of 0.4 and 0.8 s respectively.

Figure 2 (a) demonstrates the existence of the recirculation bubble distal to a circular stent strut during coronary flow deceleration. The length of the recirculation bubble was measured by identifying the negative WSS region along the arterial lumen. As can be observed in Figure 2 (b), recirculation bubbles exist distal to both square and circular cross-sectional struts. In brief, recirculation bubbles are more prominent during coronary flow deceleration, but disappear as coronary flow increases. Moreover, square strut results in a larger recirculation bubble than the circular strut. In other words, circular strut demonstrates better haemodynamic performance than square strut with identical strut thickness.

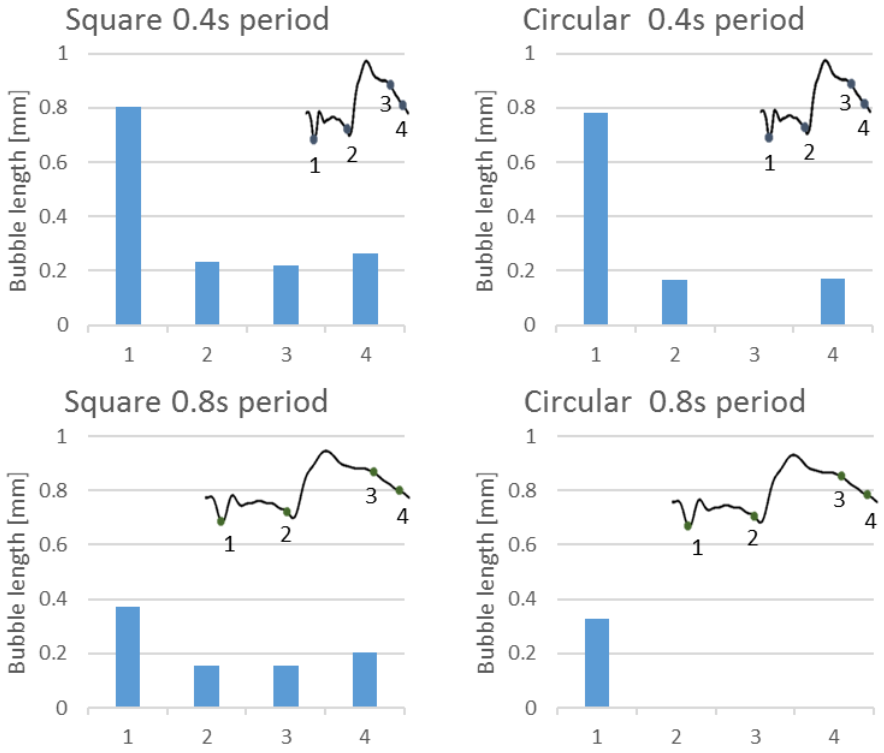


**Figure 3.** Comparison of recirculation bubble sizes at the same location of the two pulses of different periods.

To further highlight the fact that the size of the recirculation bubble is correlated to rapid flow deceleration, we quantitatively presented the size of the recirculation bubble at different flow deceleration rates and cardiac cycles in figure 3. For a specific strut cross-section profile, there is a reduction of the recirculation bubble size as cardiac cycle increases (from 0.4 s to 0.8 s). In addition, recirculation bubbles are most pronounced at point '1' of both cardiac cycles where coronary flow velocity decelerates at the highest rate. On the other hand, at points '2', '3' and '4', flow deceleration is less steep and the recirculation bubble sizes decrease. Nevertheless, the presented CFD results show that recirculation bubble size is positively correlated to the rate of coronary flow deceleration.

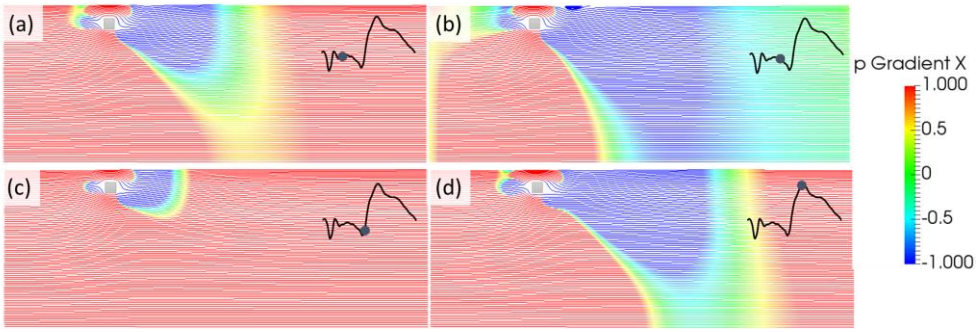


**Figure 4.** Instantaneous steamwise pressure gradient along with streamlines at different time phase in the 0.4 s period pulse of the square strut case (positive pressure gradient drives the flow from left to right). The phase is indicated in the inset with a dot.

In order to understand the physical mechanism that governs the evolution of recirculation bubbles, we carefully analyse the changes in pressure gradient field at different time for a cardiac cycle of 0.4 s.

It should be noted that the changes in pressure gradient for a cardiac cycle of 0.8 s follow a qualitatively similar trend as those in 0.4 s cycle and thus are not reported here. Pressure gradient range is set from -1 to 1 in order to clearly show the sign of the areas. In Figure 4(a), the change in coronary flow is almost zero (i.e., neither accelerating nor decelerating). The presence of the malapposed strut represents an obstacle in the near wall that affects the pressure recovery behind the stent strut. As a result, there is a small region of negative pressure gradient downstream of the strut. However, as flow starts to decelerate (see Figure 4(b), the negative pressure gradient region behind the malapposed strut gets bigger and begins to push fluid particles backwards. The presence of the malapposed strut prevents the near wall laminar reverse flow (defined by the Womersley profile [7]) and leads to the formation of a recirculation bubble. As inlet flow velocity accelerates again (Figure 4(c)), this creates a substantial positive pressure gradient along the streamwise direction that results in better pressure recovery behind the malapposed strut. This positive pressure gradient in front and behind the malapposed strut helps "wash off" the recirculation bubble. Coronary flow peaks in Figure 4(d) and rate of change of velocity approaches 0 again. As a result, the pressure gradient field becomes qualitatively similar that presented in Figure 4(a) and the pressure gradient field evolves in a similar trend as mentioned above when the flow decelerates again.

## 4. Conclusion

This study shows that the size of blood flow recirculation bubble expands as cardiac cycle decreases (i.e., a faster deceleration of inlet velocity). When flow decelerates, the malapposed stent strut prevents the laminar reverse flow (Womersley profile) near the arterial wall and forms recirculation bubble. With the same thickness and malapposition distance, circular cross-sectional stent strut always has a smaller size of recirculation bubble than stent strut of a square cross section in both 0.4 s and 0.8 s cardiac cycles, therefore, circular stent strut surpasses the square one in terms of haemodynamic performance.

## 5. References

[1] Foin N, Lee R D, Torii R, Guitierrez-Chico J L, Mattesini A, Nijjer S, Sen S, Petraco R, Davies J E, Di Mario C, Joner M, Virmani R and Wong P 2014 Impact of stent strut design in metallic stents and biodegradable scaffolds *Int. J. Cardiol.* **177** 800–8

[2] Jimenez J and Davies P F 2009 Hemodynamically Driven Stent Strut Design *Ann. Biomed. Eng.* **37** 1483–94

[3] Sprague E A, Luo J and Palmaz J C 1997 Human aortic endothelial cell migration onto stent surfaces under static and flow conditions *J. Vasc. Interv. Radiol.* **8** 83–92

[4] Dodge J T, Brown B G, Bolson E L and Dodge H T 1992 Lumen diameter of normal human coronary arteries. Influence of age, sex, anatomic variation, and left ventricular hypertrophy or dilation. *Circulation* **86** 232–46

[5] Foin N, Gutiérrez-Chico J L, Nakatani S, Torii R, Bourantas C V., Sen S, Nijjer S, Petraco R, Kousera C, Ghione M, Onuma Y, Garcia-Garcia H M, Francis D P, Wong P, Di Mario C, Davies J E and Serruys P W 2014 Incomplete stent apposition causes high shear flow disturbances and delay in neointimal coverage as a function of strut to wall detachment distance implications for the management of incomplete stent apposition *Circ. Cardiovasc. Interv.* **7** 180–9

[6] Davies J E, Parker K H, Francis D P, Hughes A D and Mayet J 2008 What is the role of the aorta in directing coronary blood flow ? *Heart* **94** 1545–7

[7] Womersley J R 1955 Method for the calculation of velocity, rate of flow and viscous drag in arteries when the pressure gradient is known *J. Physiol.* **127** 553–63